Elaboration of hydrophobic flax fibers through fluorine plasma treatment

Olivier Teraube, Léa Gratier, Jean-Charles Agopian, Monica Francesca Pucci, Pierre-Jacques Liotier, Samar Hajjar-Garreau, Elodie Petit, Nicolas Batisse, Angélique Bousquet, Karine Charlet, et al.

Elaboration of hydrophobic flax fibers through fluorine plasma treatment

Olivier Téraube [a,b,*], Léa Gratier [a,b], Jean-Charles Agopian [a,b], Monica Francesca Pucci [c], Pierre-Jacques Liotier [d], Samar Hajjar-Garreau [e], Elodie Petit [a], Nicolas Batisse [a], Angélique Bousquet [a], Karine Charlet [b], Éric Tomasella [a], Marc Dubois [a]

[a] Université Clermont Auvergne, Clermont Auvergne INP, ICCF, BP 10448, 63000 Clermont-Ferrand, France
[b] Université Clermont Auvergne, Clermont Auvergne INP, Institut Pascal, BP 10448, 63000 Clermont-Ferrand, France
[c] LMGC, Univ Montpellier, IMT Mines Ales, CNRS, Ales, France
[d] Polymers Composites and Hybrids (PCH), IMT Mines Ales, Ales, France
[e] Institut de Science des Matériaux de Mulhouse, CNRS-UMR 7361, Université de Haute-Alsace, 68057 Mulhouse, France

A B S T R A C T

In this study, the goal was to compatibilize flax natural fibers (which are inherently polar) with mostly dispersive polymers, while proposing a way to recover greenhouse gases or refrigerants such as CF_4 or C_2F_5H. Such gases exhibit a high global warming potentials (GWPs) and their recovery at the end of their lifecycle is difficult. Therefore, these two representative problematic gases were used as plasma precursor to graft fluorine atoms onto the flax fiber surface. Chemical investigation (FT-IR, ^{19}F NMR and XPS spectroscopies), demonstrates the covalent grafting of fluorine atoms at the fiber surface, that opens the route of tailoring the surface chemistry of flax fibers. These modifications induced a decrease of the fiber polarity, which allows the treated fibers to become perfectly compatible with mostly dispersive polymer. Moreover, both mechanical properties and fluorine release during fibers combustion were investigated and any negative impact was evidenced. Therefore, thanks to the plasma fluorination, the gap between the surface energies of the fibers and mostly dispersive polymer matrix was reduced improving the wettability of the fibers through an eco-friendly way. This phenomenon promising an improvement in the mechanical performance of eco-composites reinforced with these fluorinated fibers.

Keywords:
Natural fibers
Plasma
Wettability
Interface
Surface properties
Surface analysis

1. Introduction

On the actual market of materials, the objective is always to obtain more performant materials, while reducing the weight, the cost and the carbon footprint of the latter. In this context, vegetal fibers, used as reinforcement of polymer matrix to manufacture “eco-composites” are good candidates to jointly solve the above-mentioned problems. In particular, flax fibers are often considered as one of the best bio-based reinforcements for composites [1]. Indeed, their low cost next to the other reinforcement fibers (less than 2 $/Kg vs. 2–3.5 $/Kg for E-glass and 8–11 $/Kg for carbon fibers [2]) their density, lower than carbon fibers (1.4–1.5 vs. 1.7 for flax and carbon fibers, respectively), and their good mechanical performances allow them to exceed the specific mechanical properties (properties reduced to a density ρ equal to 1) of the glass fibers, and even, of a part of aramid fibers [2,3]. Therefore, all these advantages allow them to be positioned as an ideal bio-based replacement of these latter and be more and more used in the transportation industry (aeronautics, automotive, etc.) in the emerging context of the bio-economy aimed at continuing economic growth while preserving the environment and earth resources.

However, because of the large numbers of hydroxyl and carboxyl groups in their chemical structure, flax fibers, as well as the whole range of lignocellulosic materials, exhibit a high polarity γ_s^p of 26,0 mN/m whereas a dispersive component γ_s^d of 34 mN/m is typically measured [4]. Those characteristics make them difficult to wet by mostly dispersive polymer [5,6], leading to the appearance of cavities between the matrix and the reinforcement, that constitutes points of mechanical weakness; cracks can emerge and propagate under stress from those cavities [7,8]. In addition, this polarity makes them sensitive to water and moisture sorptions. Therefore, swelling and shrinkage caused by water absorption and desorption change the fiber morphology and result in cracks in the composite structure [9]. This second point limits the use of these fibers for composites employed in contact with water (boat, offshore or outdoor construction, etc.) and forces engineers to prevent

* Corresponding author at: Université Clermont Auvergne, SIGMA Clermont, ICCF, BP 10448, 63000 Clermont-Ferrand, France.
E-mail address: olivier.teraube@outlook.com (O. Téraube).

any contact of these materials with water. Most of the time, the hydrophilic character of the fibers is discussed as the main reason for the incompatibility towards the hydrophobic polymers. These terms "hydrophilic" and "hydrophobic" are often confusing because they are only related to water interaction and do not allow to rigorously describe the physical–chemical interactions that take place at the fiber/matrix interface within the composite. Therefore, notions of polarity and dispersivity will be privileged in this paper; hydrophilicity is mostly related to a high polarity, while hydrophobicity is related to a low polarity.

In order to reach the optimal performance that vegetal fiber composites are capable of promulgating, a filler/matrix compatibilization is mandatory. Thermal treatment, electric discharge or chemical treatment (acetylation, MAPP treatment, mercerization, etc.) [10] are some of the different techniques; the aim is always to adapt the fibers polarity to those of the polymer matrix, by reducing it superficially. However, nowadays industrial treatments employed to compatibilize vegetal fibers with mostly dispersive polymers are unfortunately costly, both time and energy consuming, and/or harmful to the environment and people by using toxic solvents or chemicals. New eco-friendly methods must be then developed to be fully in accordance with the concept of "eco-composite". For this purpose, novel "green" processes for achieving this compatibilization without impacting the environment must be developed [11–18] keeping in mind the necessary scale-up to an industrial scale, the additional investments and/or the development of new technologies.

On the other hand, plasma treatments, *i.e.* the use of an electrically neutral ionized gas that forms when at least one electron is no longer bound to an atom or molecule [19], are increasingly used to modify the outmost surface of various substrates [20–22]. On the other hand, depositing fluorine atoms onto the surface of lignocellulosic materials is known to decrease the polarity of the latter, and thus to increase the fiber/matrix compatibility [23,24]. If fluorine containing plasmas were first developed for etching in micro-electronics, they are currently also employed to graft fluorine or fluorine containing groups at the substrate surface to modify their reflectance or their wettability [25]. Typical fluorinating agents are SF_6, NF_3, CF_4, CHF_3, C_2F_6, C_3F_6 and C_4F_8 gases [19,26].

In the present work, we propose to use plasma fluorination treatment to make flax fibers less sensitive to ambient humidity while making them compatible with hydrophobic polymer matrices, in a sustainable and ecological way. Indeed, the treatment offers the possibility to combine a surface etching with the grafting of fluorine atoms on the surface of the plant fibers, making them less polar [27–32]. Moreover, as a gas/solid reaction, plasma fluorination is performed without toxic solvent in a closed reactor that avoids the release of toxic substances in the atmosphere. In addition, employ greenhouse gas such as CF_4, or refrigerant such as C_2F_5H, as plasma precursor would be a way to recover them at the end of the cycle. This approach of recycling these fluorinated gases in a fluorinated plasma fits perfectly into the environmental approach of the 21st century, and as employed on bio-sourced materials, *i.e.* flax fibers. The term of "eco-composite" may be properly used.

Therefore, this paper deals with two fluorinated plasma treatments based on the two environmentally problematic gases CF_4 and C_2F_5H, carried out for treatment of flax fibers. The strategy consists in covalently graft fluorine groups on the outmost surface of flax fibers in order to decrease their polar character and then to obtain more performing composites within an environmental approach. These assumptions will be confirmed, among others, by complementary characterization techniques at different levels, *i.e.* on the surface (XPS, tensiometry) and in the bulk (NMR, mechanical tests).

2. Material and methods

2.1. Plasma fluorination

Flax fibers were pieces of a February 2021 roll of FlaxTape™ (referenced L-FLAXTAPE-110–36 m^2; 90 m long 400 mm wide and 110 g/m^2 density) purchase from Eco-Technilin, cut to the size of 6x4 cm^2. Chemical composition of these fibers (dried) has been measured using ADF-NDF-ADL method, according to Van Soest [33]. Two measurements were performed, and results are summarized in Table 1.

Before each treatment, flax fibers were outgassed for at least 2 h under primary vacuum (10^{-3} mbar) at 80 °C. Treatments were then performed using Alliance Concept EVA 300 + PECVD type machine. A base pressure of 1. 10^{-6} mbar is reached using a primary and a secondary turbomolecular pump. Two fluorinated gases have been selected as precursors: tetrafluoromethane (CF_4) purchase from Messer France (99.999% purity) and pentafluoroethane (C_2F_5H) purchase from ABCR GmbH (99.0% purity). CF_4/Ar and C_2F_5H/Ar mixtures with a flow rate of 5/5 sccm (standard cubic centimeters per minute) for each gas have been used for a working pressure equal to 10^{-2} mbar. RF power was set at 150 W on the substrate holder and the duration of treatment has been chosen between 5 and 60 min. Experiments and results which have allowed to select these parameters are presented in supporting information (SI).

2.2. Characterization

Infrared spectrometry was performed using a Nicolet 6700 FT-IR (Thermo Scientific) spectrometer. Spectra were recorded in ATR mode (diamond crystal) using 32 scans and a resolution of 4 cm^{-1}.

^{19}F solid-State NMR experiments were conducted on a 300 MHz Bruker Avance spectrometer at a resonance frequency of 282 MHz. Magic-angle-spinning (MAS) probes equipped with 2.5 mm spinning modules were used for all experimentation at 30 kHz spinning rate. The acquisition sequence was composed of a single 90° pulse lengths of 3.5–5.0 µs. ^{19}F chemical shifts were externally referenced to CF_3COOH and then referenced to $CFCl_3$ ($\delta_{CF_3COOH} = -76.6$ ppm vs δ_{CFCl_3}).

X-ray photoelectron spectroscopy (XPS) measurement was carried out in order to investigate the surface composition of fibers. Experiments have been conducted on a VG Scienta-SES 2002 hemispherical analyzer which made use of monochromatic Al K_α (1486.6 eV) X-ray source radiation and an electron gun for charge effect compensation.

Spectra were fitted with Gaussian-Lorentzian component profiles after a Shirley background subtraction, thanks to the casaXPS software 2.3.18 Ltd., Teignmouth, UK and all peaks were repositioned by positioning the Csp^3 (C–C/C–H C1s line at 284.9 eV).

Optical Emission Spectroscopy (OES) characterisation of plasma is a powerful tool to identify certain species present in the gas phase [36] and thus to understand their influence on modifications of fibres properties composition.

This technique, in addition to its relatively common implementation, has the advantage of being non-destructive and provides information on radiative species in real time. In OES, element in an excited state emits a specific radiation when coming back to a lower state. The transition is characterised as following:

$$X^* \rightarrow X + h\nu \quad (1)$$

The whole photons emitted by all radiative species then constitute the optical emission spectrum. Since transition wavelengths are known for a given excited species X*, the collected spectra make possible identifying the radiative species present in the plasma.

A CCD spectrometer with an optical fibre input (Horiba scientific

Table 1
Chemical composition of dried raw fibers.

	Experimental (%)	Theoretical (%) [34,35]
Lignin	2.9 ± 0.9	2–3
Cellulose	85.2 ± 7.0	60–81
Hemicelluloses	3.9 ± 8.2	14–21
Extractives	8.6 ± 0.5	<10

iHR320 Imaging Spectrometer) was used to obtain the plasma emission spectra throughout the reaction volume and using a fused-silica window. The monitored emission lines were: the ones of argon (Ar*) at 695.5 nm, 702.9 nm, 706.5 nm; hydrogen (H_α) at 656.5 nm, oxygen (O*) at 844.6 nm, carbon monoxyde (CO*) at 297.9 nm and fluorine (F*) at 703.7 nm in addition to the molecular CF_2* lines at 587.9 nm [37]. One reprenseative spectrum is shown in SI (Fig. SI3).

In order to visualized the fiber surface at different scales, SEM observations and AFM measurements were carried out using respectively a Zeiss Supra 55VP equipped with a Gemini column and a Bruker Innova® Atomic Force Microscope equipped with a RTESPA-300 8 nm radius silicone probe (in tapping mode at 0.5 Hz). On the one hand, SEM images were recorded at a magnification of 2000x with a working energy of 3KeV. On the other hand, AFM data have been acquired on a 2 μm^2 surface.

Fluorination treatment is expected to modify the surface tension of fibers. As this evolution is classically measured using the "sessile drop" technique [38], it is not possible to place liquid drops on fiber because of teir cylinder shape. Thereby, in order to determine the surface energy of our flax fibers, a tensiometric method was carried out. Indeed, among the different techniques develop along the age [39–42], this technique appears as the most convenient. First described by Qiu *et al.*[40], it is based on the use of a Wilhelmy balance and the Wilhelmy relationship:

$$F = \gamma_L p \cos\theta \tag{2}$$

where F is the capillary force (mN), p (m) the wetted length, θ (°) the contact angle and γ_L (mN/m) the surface tension of the liquid.

The procedure carried out in this paper was the same than the one described in [43].

Measurements were performed using a Krüss K100SF tensiometer. A single fiber was immersed in n-hexane which is considered as totally wetting (θ = 0). From there, the Wilhelmy equation allowed the wetted length of the fibers to be determined. Then, knowing the wetted length and the tabulated γ_L, the contact angle is determined using equation Eq. (3) by measuring the force F exerted by the liquid under study on the fiber.

Thereby, when two different liquids water and diiodomethane were considered, the Owens-Wendt equation (Eq. (3)) allows the polar and the dispersive component of the surface energy of fibers to be identified [44].

$$\frac{\gamma_{liq}(1+cos(\theta))}{2\sqrt{\gamma_{liq}^d}} = \sqrt{\gamma_{fibre}^p}\left(\frac{\sqrt{\gamma_{liq}^p}}{\sqrt{\gamma_{liq}^d}}\right) + \sqrt{\gamma_{fibre}^d} \tag{3}$$

Fluorine gas release during combustion of the sample must be quantified, because of the hazardousness of these compounds. To perform this measurement, a set-up combining an ATG analysis (STA Netzsch Jupiter F3 analyzer) with a mass spectroscopy analysis of the released gases (Netzsch Aeolos Quadro) was used with a heating ramp of 10 K min^{-1}.

Finally, to evaluate the impact of the plasma fluorination treatment on the mechanical properties of flax fibers, tensile tests of fibers were performed in compliance with the NF T 25–501-2 standard [45] on an Instron 5543 tensile testing machine equipped with a 50 N load cell and pneumatic grips.

Tests were performed according to the following sequence on (at least) 50 samples for each sample:

- Single flax fibers have been glued on a Kraft-paper frame with a central hole of 10 mm (gauge length);
- Average fiber diameter was obtained considering 3 measurements of the diameter under microscope at 1000x magnification;
- Kraft-paper frame with the fibers was placed into the pneumatic grip, then frame edges were cut and the test was started with a constant crosshead displacement rate of 1 mm/min.

3. Results and discussion

3.1. Presence of fluorine and chemical change

FT-IR experiments were performed for fibers resulting from all fluorination durations of both gas mixture; results (displayed in supporting information, Fig SI2) evidence the presence of fluorine atoms contently grafted at the outmost surface of flax fibers. Indeed, deconvolution of IR spectra was performed to evidence the appearance of several carbon–fluorine vibration bands in between 1000 and 1400 cm^{-1} (wine color lines in Fig. SI2). As this wavenumber range is related to the C-F stretching band area [46], these peaks evidence the formation of covalent C–F bonds; the higher the area under the wine color line, the higher the fluorination rate. Because only the outmost surface is treated, the intensities of those bands are weak and a definitive conclusion is permitted only for the optimum treatment conditions. The FT-IR data, discussed in supplementary information (SI), allow those conditions to be selected. In accordance with the works of Xie *et al.* [32] dealing with wood plasma fluorination, the presence of argon in addition to CF_4 or C_2F_5H is necessary to observe the C-F bands (see SI). We assume that argon plays 2 key roles: on the one hand, it allows to clean the surface of our substrate and create free radicals at the fibers surface, which may react with plasma radicals. On the other hand, the presence of argon dilutes fluorinated species in the plasma and decreases the probability of their recombination, resulting in the increase of the number of molecules that come in contact with the substrate. In other words, the reactivity of fluorinated species towards the fibers is increased. The second conclusion of the preliminary study is the efficiency of low gas mixture flow, *i.e.* 5/5 SCCM, which will be systematically used with power of 100 W.

Fig. 1 displays the C1s XPS deconvolution of raw and some fluorinated sample. Spectrum of the pristine fibers can be decomposed in 4 components. The first peak at 284.9 eV was assigned to Csp^3 (C–C/C–H) which composed the natural polymers of flax fibers (cellulose for example) thus Csp^2 of lignin aromatic cycles. Then, at 286.6 eV, a second peak can be observed that corresponds to carbon–oxygen groups where the carbon form a single bond with the oxygen (C-OH, C-O-C or Phenyl-OH). Thereafter, the contribution at 288 eV is still related to carbon–oxygen groups but forming a double bond between them (C = O for example). Finally, a peak evidences to the presence of Csp^3 belonging to ester and carboxyl groups [47–50].

After the CF_4/Ar and the C_2F_5H/Ar fluorination treatment, a new contribution makes its appearance at 688 eV on the XPS survey and proved the covalent grafting of fluorine atoms on flax fibers [67]. Table 2 summarizes the atomic percentage of chemical elements present on the fibers surface. Oxygen and carbon are the two main atoms that constitute raw flax fibers. After the fluorination treatment realized with the CF_4/Ar plasma first, the atomic ratio F/C moderately increases to 0.35 after 40 min of treatment before increasing much more significantly up to 0.81 after 60 min of fluorination. This showed that, between 40 and 60 min, fluorine atoms are more efficiently grafted. In the meantime, O/C ratio changes between 0.21 and 0.15. These small variations are probably due to the natural heterogeneity of a vegetal material rather than an effect of the treatment on the fibers 'oxygen. Thereby, O/C ratio seems stable, sign that fluorination with CF_4 does not affect the oxygen quantity present within the material. Concurrently to the appearance of the F1s contribution, 5 peaks corresponding to C-F bonds appear in the C1s spectrum and their assignments are displayed in Table 2, according to [47,64–66,68–70].

Regarding C-F groups present on CF_4 treated fiber surface (Table 3), we can notice that CF groups are in majority up to 40 min. After 60 min, a clear increase in the amount of CF_2 and CF_3 grafted groups is observed.

On the other hand, with C_2F_5H/Ar plasma, the atomic ratio F/C reaches 0.63 after only 10 min of treatment and further increase up to 0.82 after 40 min (Table 3). Thereby, in comparison with CF_4 based plasma, the use of C_2F_5H allows a larger amount of fluorine to be grafted

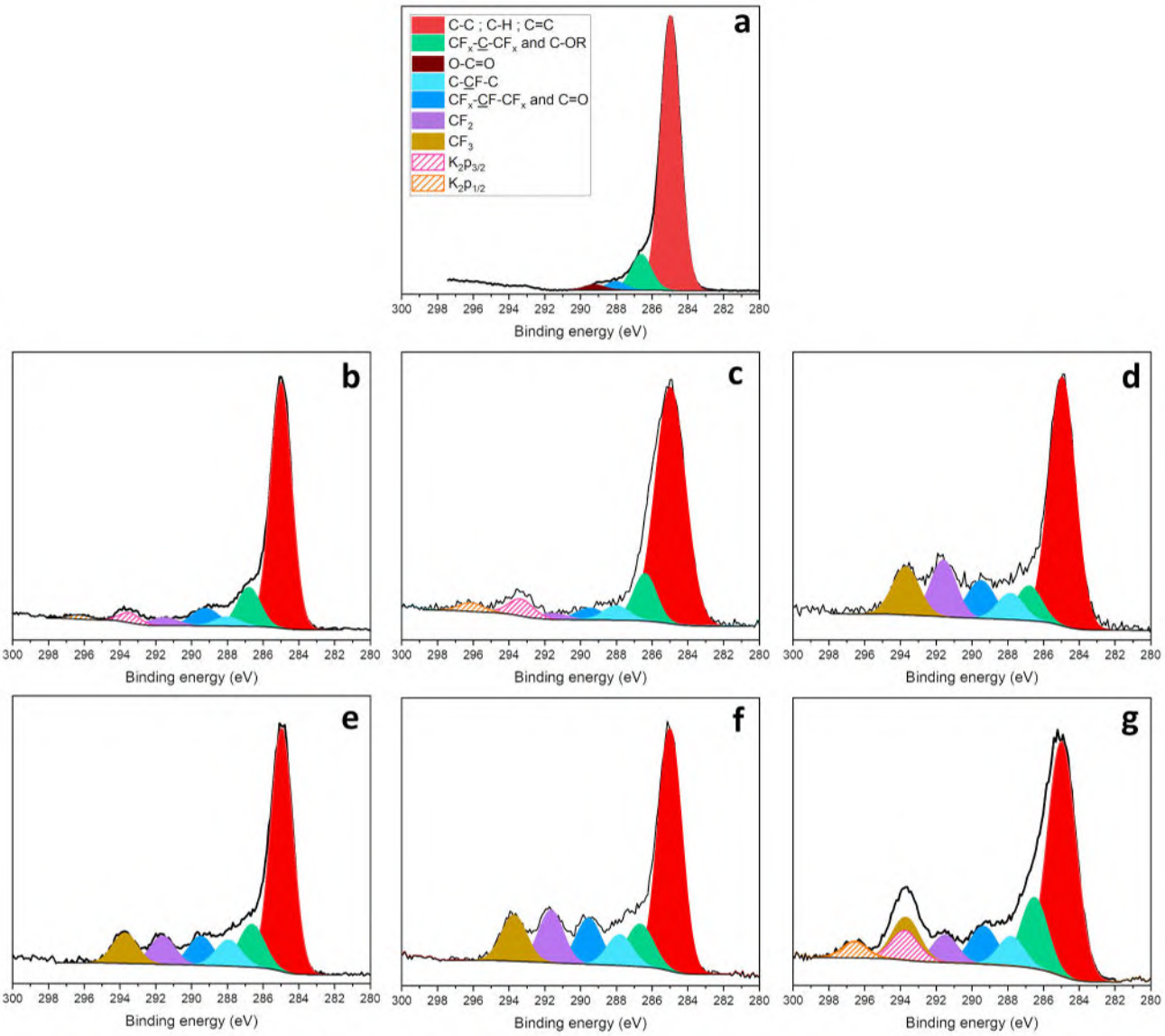

Fig. 1. C1s XPS spectra of flaw fibers (a) raw, (b) CF_4/Ar – 10 min, (c) CF_4/Ar – 40 min, (d) CF_4/Ar – 60 min, (e) C_2F_5H/Ar – 10 min, (e) C_2F_5H/Ar – 40 min, (g) C_2F_5H/Ar – 60 min.

Table 2
Assignments of the C1s contributions appeared after the fluorination treatment in the C1s spectrum according to [47,64–66,68–70].

Binding energy (eV)	286.6	287.2	288.8	291	293.6
Assignment	CF_x-C-CF_x	CH_x-CF- CH_x	CF_x-CF- CF_x	CF_2	CF_3

Table 3
XPS surface atomic composition of raw and plasma fluorinated flax fibers.

	Atomic percent (%)				Atomic ratio	
	C	O	F	Bi	O/C	F/C
Raw	82.3	17.7	/	/	0.21	/
CF_4/Ar-10 min	70.1	11.0	18.3	0.6	0.15	0.26
CF_4/Ar –40 min	62.4	12.6	21.9	3.1	0.20	0.35
CF_4/Ar –60 min	52.0	4.4	42.6	1.0	0.18	0.81
C_2F_5H/Ar –10 min	56.4	6.5	35.7	1.3	0.12	0.63
C_2F_5H/Ar –40 min	51.9	4.4	42.8	0.9	0.08	0.82
C_2F_5H/Ar –60 min	51.1	8.2	40.3	0.4	0.16	0.79

in a shorter time. In parallel, the O/C ratio remains constant, as observed with CF_4/Ar plasma. Concerning the C-Fx groups (Table 4), the amount of CF_3 and CF groups are stable along the time, at the opposite of the quantity of CF_2 which starts to increase from 4.2 to 6.0 before decreasing to 2.8. If the reason of this decreased have not been identify, it is clear that whatever the fluorination duration C_2F_5H induced approximately the same chemical grafting. On the contrary, with CF_4 gas, the composition (and probably the thickness) of the fluorine layer is time

Table 4
Percentage of carbon based groups from XPS C1s spectra of raw and fluorinated flax fibers.

	Group percent (%)			
	CH/CC	CF	CF_2	CF_3
Raw	56.7	/	/	/
CF_4/Ar-10 min	50.8	6.9	2.2	1.0
CF_4/Ar –40 min	47.1	4.6	1.1	1.4
CF_4/Ar –60 min	28.7	7.6	6.3	5.6
C_2F_5H/Ar-10 min	32.8	8.3	4.2	4.5
C_2F_5H/Ar –40 min	26.2	9.0	6.0	5.4
C_2F_5H/Ar –60 min	27.2	7.4	2.8	4.8

dependent, probably due to different ways of fluorine grafting.

In addition to the 5 peaks presented in Table 2, 2 additionnal contributions (293.8 and 296.6 ev) are observable in the C1s area. As explained on a previous paper about the direct fluorination with F_2 gas of the same type of fibers [43] these contribution could not be attributed to any C-F bond because of their very high binding energy. Indeed, according to [51], this binding energy is more in line with that of $K_{2p2/3}$ and $K_{2p1/2}$ with a spin–orbit coupling of 2.8 and thus reflect the presence of potassium (K) at the fibers surface after the fluorination treatment. A hypothesis that we have previously formulated [43] to explain the presence of potassium at the flax fiber surface when they are fluorinated is that potassium has always been present within flax fibers, as already observed in different papers [52,53]. Thereby, because of the high affinity of K with F (to form KF) and through the action of the fibers pretreatment 80 °C under vacuum, potassium ions would have migrated into the surface of the fibers (where the fluorine is present). Furthermore, two other components appear on the general survey after the fluorination treatment at 160.0 and 165.3 eV. These peaks, with respectively correspond to the bismuth $Bi_{4f7/2}$ and $Bi_{4f5/2}$ are due to a due to bismuth pollution because of previous experimentation that have been realized in the same reactor.

To better understand the fluorination mechanism and at another scale, ^{19}F NMR measurements were carried out; data presented in Fig. 2 are representative of the bulk of the fluorinated layer contrary to 8–9 nm thickness for XPS.

Flax fibers and all lignocellulosics materials are mainly composed of bio-polymers (cellulose, lignin and hemicelluloses), and it is well known that CF_x plasma allows to graft CF_y (CF_3, CF_2 or CH_yF (y = 0, 1 or 2) groups at the polymer surface [31]. Because of the deshielding effect of ^{19}F nuclei, the chemical shifts of CF_3 groups are the highest (about −40/−90 ppm), then CF_2 groups (about −100/−155 ppm) and finally CH_yF (y = 0, 1 or 2) groups (in between −160 and −250 ppm). To highlight these areas, they have been greyed in Fig. 2.

Considering the CF_4/Ar case first, we do not notice important change in NMR spectra while the fluorination duration increases. Indeed, the CF_4/Ar-30 min spectrum is pretty similar to the 5 min one, sign that only few changes in the chemical structure of the fluorine layer occurred. After 40 min and more firmly after 60 min of plasma fluorination, the appearance of the line for CF_3 groups evidences their presence. Two phenomena may explain this fact: the appearance of $CF_3^{\bullet}$ radicals in the plasma after 40 min, which would be grafted at the outmost surface of fibers or the beginning of degradation. Indeed, if $F^{\bullet}$ reacts on C-CF_2-C a disruption of C–C bond occurs and CF_3 group is formed, as frequently observed with F_2 fluorination [54–56]. However, because CF_3 groups do not appeared progressively with time, degradation phenomenon seems more likely.

For the case of C_2F_5H series, once again only few changes of spectra are observable when increasing the duration of the plasma fluorination treatment. Nevertheless, we can denote an important difference between CF_4/Ar and C_2F_5H/Ar treatments. Indeed, with this latter gas, peaks which are assigned to CF_3 groups appeared on NMR spectrum for short duration (already present after 5 min of fluorination) and increase in intensity progressively. This phenomenon, not observed on CF_4/Ar samples, denotes a continuous grafting of CF_3 all along the time. XPS data gives a nearly constant relative content of CF_3 groups when C_2F_5H/Ar is used (Table 3) evidencing the saturation near the fiber surface. The increase seen by NMR is related to an propagation of the fluorinated layer with thickness higher than 8–10 nm. In addition, for the C_2F_5H case, the signal-to-noise ratio is much higger for longer fluorination time than for shorter. This is in good adequation with the increase of the positive contribiution due to fluorine, previously observed on FT-IR spectra.

Moreover, ^{19}F NMR spectra were recorded with 512 scans to obtain a suitable signal-to-noise ratio. However, even after this consequent number of scan the signal is very noisy, and given the 100% isotopic abundance of ^{19}F and its high relative sensitivity (0.82), these conditions reflect that fluorine is only present in small quantities within the fibers. Thereby, the main part of grafted fluorine atoms would be at the

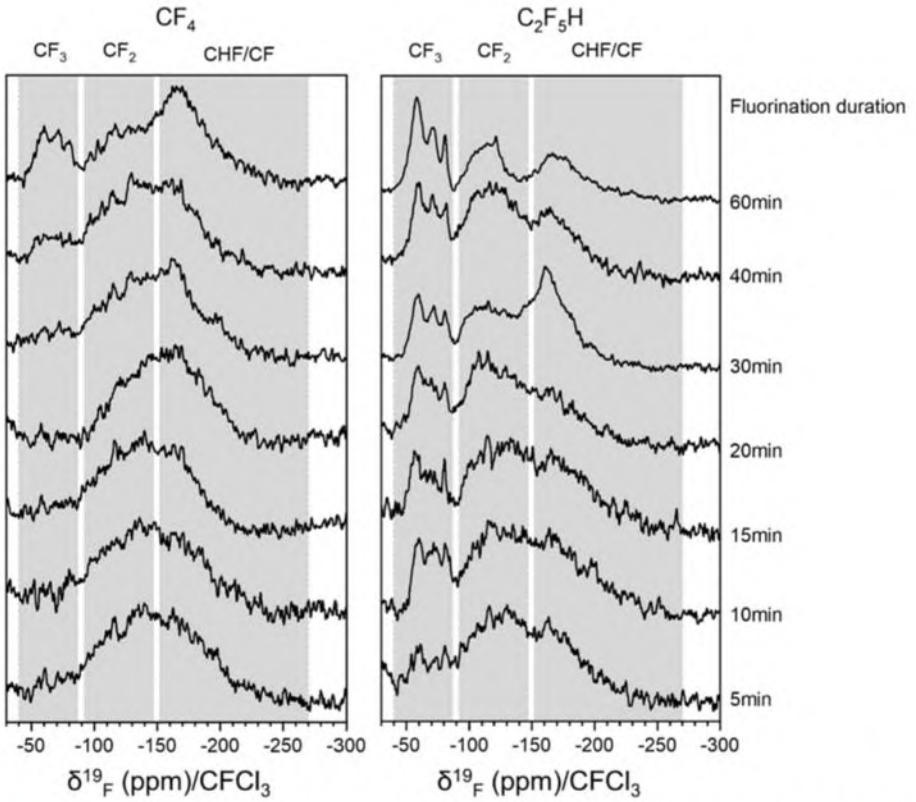

Fig. 2. ^{19}F solid-state NMR spectrum of plasma fluorinated flax fibers with CF_4/Ar (left) and C_2F_5H/Ar (right).

outmost surface of fibers.

To better understand the reason of the difference in the fluorine grafting, the chemical composition of the 2 different plasmas (CF_4/Ar and C_2F_5H/Ar, with a flow rate $\Phi_{Ar}=\Phi_{CF4}=\Phi_{C2F5H}$ = 5 SCCM) was analyzed by optical emission spectroscopy (OES). The normalized ratio of fluorine and hydrogen group to argon line intensity (I_F/I_{Ar}, I_{CF2}/I_{Ar}, and I_H/I_{Ar}) are presented in Table 5 (for each normalisation the 706.5 nm argon peak has been chosen as it has the highest intensity).

None of plasma mixture contains CO or O group/atoms (coming from residuals gas) in its composition thank to low presure. Thereby, no pollution from the ambiant atmospere has been possible. The CF_4 based plasma does not contain $H^\bullet$ radicals contrary to C_2F_5H based one. This $H^\bullet$ radical is thus mainly the signature of $CHF_x^\bullet$ type (x = 1 or 2) however, a rupture of the C–H bond is also possible, even though less probable due to the higher strength of this bond in comparison with C–C bond (Table 6).Therefore, H* band is both due to the presence of CHF_x* and H*. In the other hand, the relative intensity of F and CF_2 are pretty similar whatever the plasma. It is to note that the emission bands of CF_3 and other similar large molecules are out of our OES spectrometer range (250–850 nm). The emission spectra of $CF_3^\bullet$ radicals is in the range 100–150 nm [57].

According to mass spectroscopy experiments and on bond energy of C–C, C–H and C-F bonds (Table 6), Agraharam *et al.* [58] have reported that the primary dissociation of the monomer in the C_2F_5H/Ar plasma are:

$$CF_3CHF_2 + e^- \rightarrow CF_3^\bullet + CHF_2^\bullet \quad (4)$$

$$CF_3CHF_2 + e^- \rightarrow CF_3CHF^\bullet + F^\bullet \quad (5)$$

Afterthat, $CF_3CHF^\bullet$ may be disociated as following, because of the weekness of the C–C bond:

$$CF_3CHF^\bullet + e^- \rightarrow CF_3^\bullet + CHF^\bullet \quad (6)$$

Further fragmentation may occur:

$$CF_3^\bullet + e^- \rightarrow CF_2^\bullet + F^\bullet \quad (7)$$

$$CF_2^\bullet + e^- \rightarrow CF^\bullet + F^\bullet \quad (8)$$

The C_2F_5H based plasma is mainly composed of $CF_3^\bullet$, $CF_2^\bullet$, $CF^\bullet$, $F^\bullet$, $CHF_2^\bullet$ and $CHF^\bullet$ radicals. However, still according to Agraharam *et al.* [58], a majority of the free fluorine radicals $F^\bullet$ in the plasma are, in their case, scavenged as HF and CF_4. However, we have a working pressure 10 times lower than that of the publication, with means 10 times less chance that a gas phase recombination occurs. Thereby, in our case, $F^\bullet$ may exist in the plasma. However, still because of our low pressure, the probability for a molecule to be impact 2 times by an electron is very low, therefore reactions presented in Eqs. (6) (7) and (8) are not very likely. Therefore, the main reaction mechanism consists of a grafting of the radicals: $CF_3^\bullet$, $CHF_2^\bullet$, and to a lesser extent $F^\bullet$, $CF_3CHF^\bullet$ and $CHF^\bullet$, which would all react with fiber surface activated by Ar^+ etching; A very large amount of different chemical environment (CF, CHF, CF_2, CF_3, CF_3CHF) are formed on the fiber surface. In addition, these radicals are present in the plasma as soon as its ignition (Table 5). Moreover, because of the large amount of radicals present in the plasma, fluorine radicals $F^\bullet$ in the system are not in the majority, that may limit the degradation phenomenon that can be observed with direct fluorination for example [54,55,59].

Table 5
Plasma normalized ratio of chemical group to argon line intensity (for each normalisation the 706.5 nm argon peak has been chosen as it has the highest intensity).

	F	CF_2	H	CO	O
CF_4/Ar	0.29	0.31	/	/	/
C_2F_5H/Ar	0.27	0.22	0.53	/	/

Table 6
C–C, C–H and C-F bond energy (according to [81]).

Bond	Energy (kJ/mole)
C–C	406
C–H	431
C-F	523

On the contrary, because CF_4 is only composed of C-F bond, the only decomposition mechanism of CF_4 is the one described below [37]:

$$CF_4 + e^- \rightarrow CF_3^\bullet + F^\bullet \quad (9)$$

$$CF_4 + e^- \rightarrow CF_2^\bullet + 2F^\bullet \quad (10)$$

$$CF_4 + e^- \rightarrow CF^\bullet + 3F^\bullet \quad (11)$$

In addition, CF_2 and CF may be formed directly from one single electron impact with enough energy (Eqs. (13) and (12)):

$$CF_4 + e^- \rightarrow CF_2^\bullet + F^\bullet \quad (12)$$

$$CF_4 + e^- \rightarrow CF^\bullet + 3F^\bullet \quad (13)$$

The plasma would be composed of $CF_x^\bullet$ and especially $F^\bullet$ radicals. On ^{19}F NMR and XPS spectra, a constant evolution of CF and CF_2 is observed for short duration and CF_3 groups appeared only after 40 min *via* a degradation phenomenon as for the case of the direct fluorination of flax fibers using F_2 [43]. The common reactive species between plasma and direct fluorination is $F^\bullet$ because F_2 is dissociated into two $F^\bullet$ on the fiber surface. Thereby, fluorination by CF_4 plasma exhibits similarities with the direct fluorination by F_2, in particular the grafting of CF_2 groups. Moreover, this indicates that the CF_4/Ar plasma is almost exclusively composed of $F^\bullet$ and $CF_2^\bullet$, $CF_3^\bullet$, $CF^\bullet$.

The comparison of XPS and NMR data evidences that C_2F_5H/Ar plasma fluorination allows to permanently increase the thickness of the fluorinated layer, contrary to the CF_4/Ar plasma fluorination. This may be explain by the fact that, in the CF_4/Ar plasma, fluorination (*i.e.* the addition of fluorinated groups on the substrate surface) and decomposition occurs simultaneously, preventing the thickening.

3.2. *Impact of fluorination*

In order to optimize the physico-chemical analyses carried out to study the impacts of plasma fluorination, we decided to focus our investigations on the optimum fluorination times. To define them, we have chosen to consider as optimum, the treatments which allowed to graft a maximum of fluorine on the whole depth of the fibers (not only on the surface). For that, we were interested in FT-IR spectra, and more particularly in the area between 1000 and 1300 cm^{-1}, where the vibrational bands of C-F bonds appear. The higher the intensity of this zone, the higher the amount of fluorine. Thereby, as these maximums are respectively reached after 10 and 40 min of CF_4 and C_2F_5H fluorination, these two times will be considered as the optimum fluorination times (more information available in Supporting Information).

3.2.1. *Wettability*

Presence of fluorine on a material surface is known to reduce its polarity [23,26,26,55,60]. However, Hansch parameters translate the gain in "polarity reduction" of a substituent when they are positive; the values are 0.14 and 0.88 for F and CF_3, respectively (0 for H) [61]. Therefore, because of the difference in fluorinated layer chemical composition, previously observed, a difference in fibers' polarity should be observed between treated fibers.

To identify and quantify changes provided by the two treatments on fibers, contact angles using the Wilhelmy balance technique were measured with water and diiodomethane and, thanks to Owens and Wendt equation, the surface energies as well as the polar and dispersive

components were calculated for flax fibers fluorinated with CF_4/Ar gas mixture (5/5 SCCM) power of 150 W for 10 min and C_2HF_5/Ar gas mixture (5/5 SCCM), power of 150 W for 40 min.

For all kind of fibers, *i.e.* the CF_4/Ar-10 min fluorinated sample or the C_2F_5H/Ar-40 min one, the polar component is significantly diminished by the fluorination treatment, from 19.1 ± 9.0 mN/m for raw fibers to 1.8 ± 2.4 mN/m and 2.8 ± 3.4 mN/m, respectively. The similarity of the polarity values shows that the amount of CF_3 appears as a secondary parameter for the surface polarity. Indeed, similar final states are achieved regardless the CF_3 relative content despite very different Hansch parameters. This phenomenon is in agreement with those from prior studies that have investigated effects on surface tension of the plasma fluorination treatment applied on different substrate [62,63]. Indeed, all these author have observed a reduction of their substrate's polarities.

On the contrary, the dispersive component γ_s^d remains nearly constant after the treatment; only slight decreases from 22.5 ± 2.0 mN/m to 21.9 ± 3.2 mN/m and to 17.8 ± 1.1 mN/m respectively for the CF_4-10 min and the C_2F_5H-40 min fibers are observed. Differences are non-significant according to the experimental uncertainties.

When further looking at the error bar value, one may observe that the polar component of both fluorinated sample is more homogeneous than that of raw fibers; vegetal fibers being natural materials and therefore intrinsically heterogeneous [64]. Compared to raw fibers, plasma fluorinated fibers exhibit a lower standard deviation of the measured surface energy. This data allows to postulate that the plasma fluorination treatment reduces natural variations in surface tension between vegetal fibers. In other words, surface energy is more homogenous, like synthetic fibers, which may attract an industrial interest since "standardized" materials are easier to implement.

Still dealing with experimental uncertainties we observe on Fig. 3, that the error bar of the polar component of treated fibers goes below 0mN/m. This is, of course, due to how the relative error (standard deviation from the mean) is calculated. Polar (and dispersive) energy cannot be negative.

In any case, despite the differences in chemical composition of the fluorinated layer, there is a very similar effect on wettability. Both optimized treatments allow the polarity of flax fibers to be decreased close to 0. Therefore, both treatments would allow flax fibers to be compatibilized with mostly dispersive polymer matrix.

3.2.2. Morphological changes

Plasma treatment, as all other surface treatment is known to act on the surface morphology of the substrate [20,32]. Different surface modifications may occur, *i.e.* degradation, etching, swelling, delamination. The presence of asperities on the filler surface of the filler is generally beneficial in the context of composite materials because they allow to create mechanical interlocking sites for the polymer matrix, reinforcing the adhesion between the fibers and the matrix. On the contrary, if the surface roughness is too pronounced, it turns into degradation and decrease the fiber wettability or reduce the effect of mechanical anchoring. In order to determine in which case the fibers are after fluorination, *i.e.* low or high roughness, SEM and AFM pictures were recorded (Fig. 4 and Fig. 6 respectively).

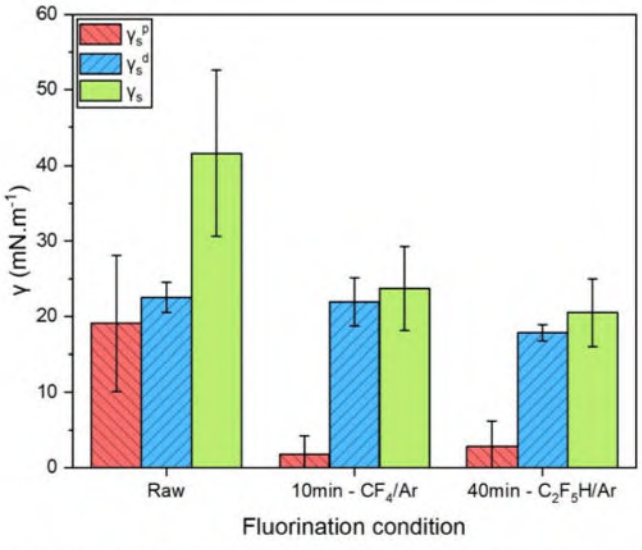

Fig. 3. Polar, dispersive and total surface energy of optimized plasma fluorinated flax fibers.

For Ar treated fibers only, we clearly observe an important surface roughness, evidencing that Ar in the plasma etches the fibers surface and probably activates it with presence of radicals due to the etching (see Fig. 7 for a schematic view). However, after the C_2HF_5/Ar treatment, no significant modification appears on SEM pictures (2000x of magnification) whether the treatment duration. For CF_4/Ar treatment contrary to the literature that reports etching with CF_4 [49], no huge degradation appears for the majority of fibers. Nevertheless, a few treated fibers exhibit a surface etching (Fig. 5). AFM confirms those observations at nanometric scale (Fig. 6). Raw fibers exhibit a surface roughness with Ra = 21.2 nm and Rq = 28.0 nm. After the CF_4/Ar plasma treatment, the values of Ra and Rq are almost identical ($Ra_{CF4/Ar}$ = 19.7 nm and $Rq_{CF4/Ar}$ = 26.2 nm). Although the etching due to Ar in the plasma (Fig. 5), the final roughness does not increase. According to [49] that evidenced etching with CF_4 plasma, the only explanation is a smoothing of rugosity due to the Ar etching by a decomposition process simultaneously to the fluorination in CF_4/Ar plasma. Etching with CF_4 plasma results in the release of CF_4 and C_2F_6 gases. In minatory regions, both etchings with Ar and fluorination superimpose resulting in a huge roughness (see Fig. 6).

On the other hand, fibers treated with C_2F_5H/Ar plasma exhibit an increase of the surface roughness since $Ra_{C2F5H/Ar}$ = 27.5 nm and $Rq_{C2F5H/Ar}$ = 33.6 nm (Fig. 6). The C_2F_5H/Ar plasma induced an etching at the nanometric scale. Either the etchings with Ar and C_2F_5H/Ar superimpose or the decomposition during fluorination is weak.

Therefore, because of its higher scale roughness, C_2F_5H/Ar treatment seems more promising in order to make composites, because it would allow to bring fiber/matrix mechanical anchoring. Indeed, this plasma etching of natural fibers have already realized on different fibers and have, in any case, improved the mechanical performance of composites (flexural, tensile, etc.) made from different techniques [65–68].

3.2.3. Mechanical properties

Considering that the surface of flax fibers has been changed both in composition and roughness, mechanical properties may be also affected. In order to investigate this point, single fibers tensile tests were carried out in order to extract the modulus (E), ultimate tensile strength (σ_m) and the percentage of maximal elongation (A%) (Fig. 8).

First and foremost, we have to discuss about the high standard deviation observable on the results of single fibers tensile tests (up to 50%). Such a behavior is owed to the natural heterogeneity of vegetal fibers [43,64,69] and explain why the NF T 25–501-2 standard [45] requires 50 fibers to be tested.

It is well accepted that surface modification causes changes in rupture properties, *i.e.* ultimate tensile strength and percentage of maximal elongation, because they are dependent on the material surface. On the contrary, Young's moduli which rather reflect bulk properties of the fibers, should not be affected by the surface modification of fibers.

As expected, a significant decrease of the ultimate tensile strength is measured for both series. Indeed, if for raw fibers, it is around 500 MPa (Fig. 8b), after the fluorination treatment the value decreases to around 305–370 MPa. The percentage of maximal elongation also significantly decreases from 3% to 1.7–2% (Fig. 8c). Surprisingly, Young's moduli (Fig. 8a) is also negatively affected by the treatment, with a decrease from 36GPa to a mean value about 25GPa. The exact reason for this phenomenon is not known at this step. Some references [70,71] report

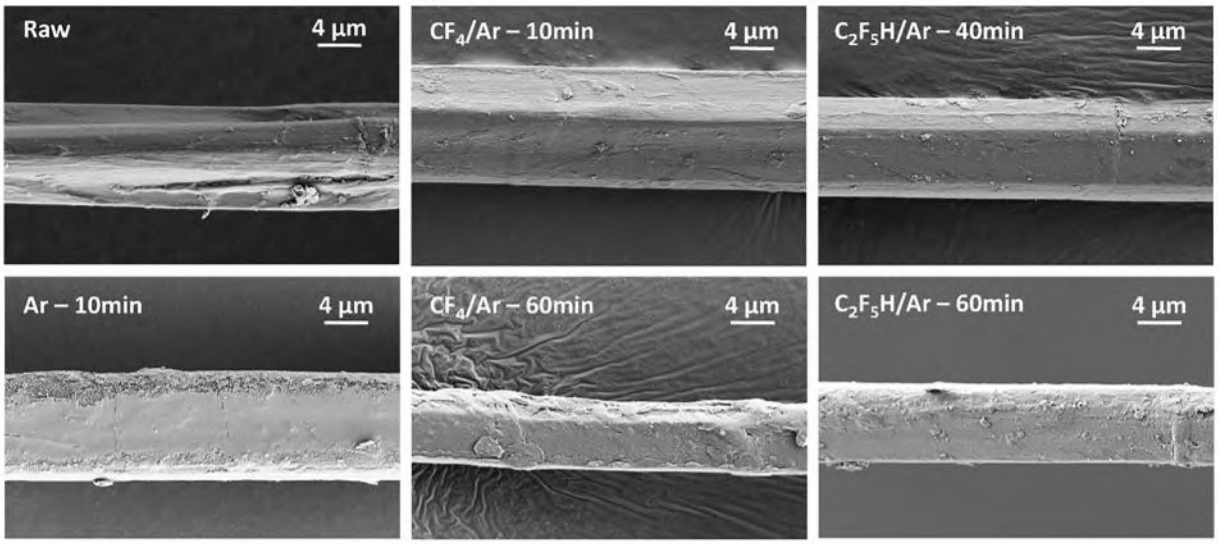

Fig. 4. SEM pictures of raw and plasma fluorinated flax fibers.

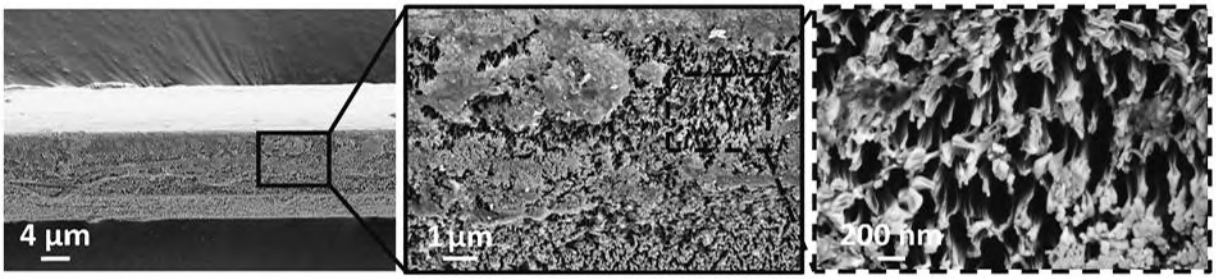

Fig. 5. SEM pictures of etched fibers by CF_4/Ar-10 min plasma treatment and zoom on etched area.

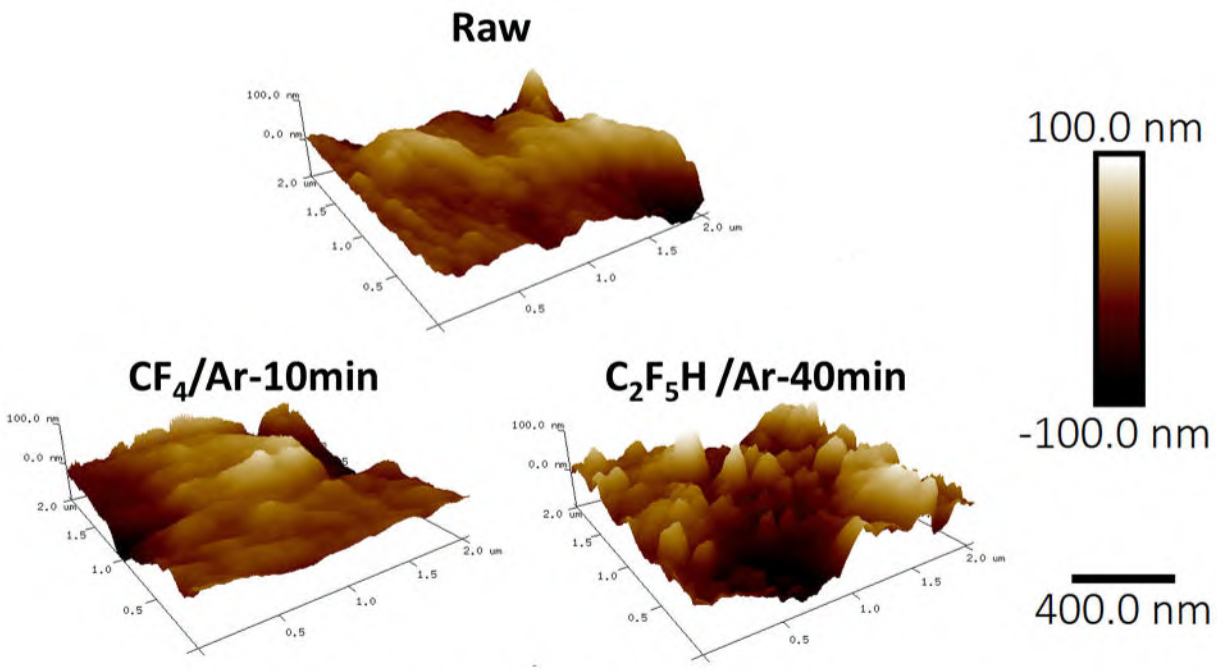

Fig. 6. AFM pictures of raw and treated flax fibers.

that the fiber porosity is open and could act as an access to the bulk for plasma. The unexpected variations in Young's modulus could be related to these changes via the porosity.

By comparing the effects of the two plasma CF_4/Ar and C_2F_5H/Ar, similarities are noted, especially with regard to ultimate tensile strength and maximal elongation. More versatility between the 2 treatments is

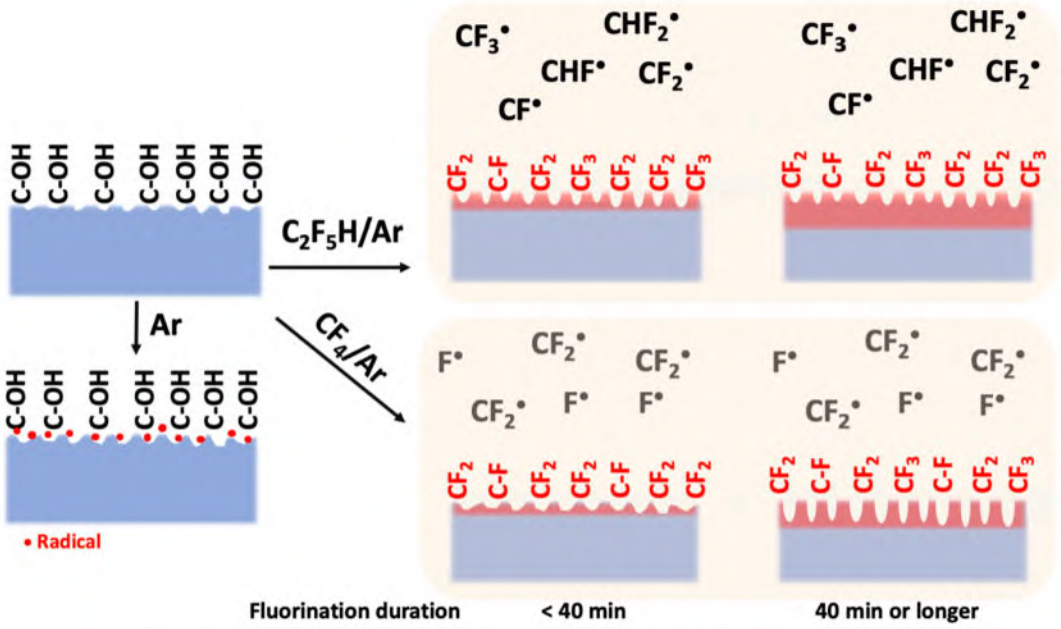

Fig. 7. Schematic view of the fluorination mechanism in C_2F_5H/Ar and CF_4/Ar plasmas.

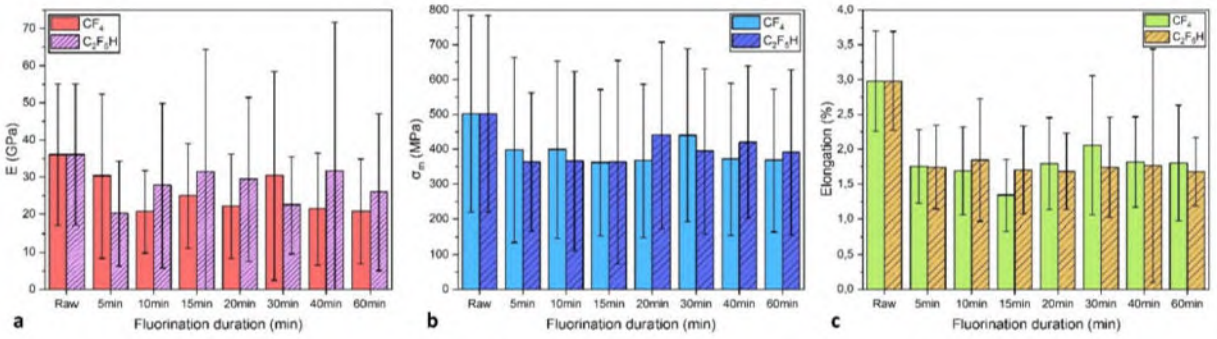

Fig. 8. Evolution of the fiber mechanical properties with the plasma fluorination duration: (a) Young's modulus; (b) Ultimate tensile strength; (c) % of maximal elongation.

observed on Young's modulus. Therefore, as already observed on wettability of treated fibers, the optimized plasma fluorination seems to occur regardless the gas although the difference in surface chemistries, *i.e.* more CF_3 groups with C_2F_5H/Ar. However, as already demonstrated by Liotier *et al.* [72] even if fibers mechanical properties are weakened by a given treatment (thermal treatment in their case), as long as the treatment improves the fiber wettability by a given polymer, the overall mechanical properties of the final composite is still improved, because of the reduction of cavities within the material. Then, the decrease of mechanical strength is probably not detrimental in view of the intended application in composite manufacturing.

3.3. *Thermic analysis and fluorine release*

Thermogravimetric analysis allows, on the one hand, the thermal behavior of the fibers to be observed in order to know if the thermal stability was modified by the treatment and, on the other hand, both the extent and the nature of the fluorinated gases emitted during a combustion to be highlighted. The second objective is made possible by using a gas spectrometer to analyze gases released during the combustion. TG curves (solid line) and the evolution of the intensity of two specific mass peaks, *i.e.* m/Z = 19 (link to F fragments and presented with dash-dot-dot line) and 69 (assigned to CF_3 fragments and presented with dash line), are plotted as a function of temperature in Fig. 9, for raw

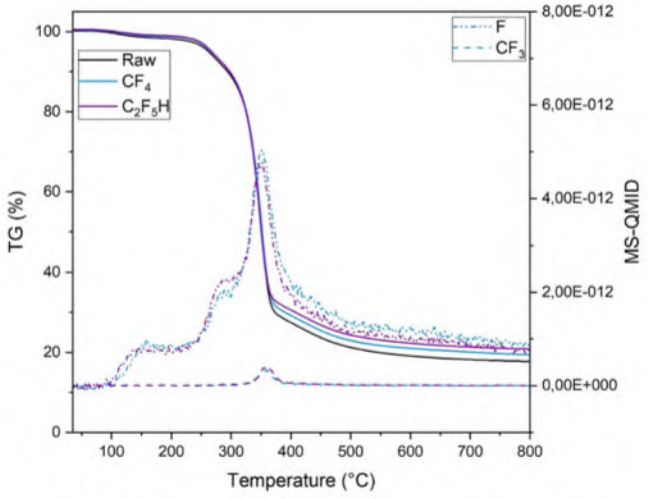

Fig. 9. ATG-MS curves for raw and plasma fluorinated samples.

and optimized fluorinated samples. Only these two peaks are represented because of the absence of big fragment on the global MS spectra, evidencing that C-F bonds are broken rather than the departure of large

gas fragments (CF_4, C_2F_6, etc.).

Concerning the TGA part, whatever the plasma type, the treatment did not significantly modify the thermal properties of the fibers, since very slight differences between the curves is noted. The thermal degradation is therefore not impacted by the plasma fluorination in agreement with its surface character.

For the MS part, after treatment with the two gases, a tiny amount departure of CF_3 is observed around 350 °C, but in derisory quantities. Departure of F atom is also observed; at temperature less than 200 °C, the first increase before stabilization corresponds to the departure of physisorbed fluorine on flax fibers surface. Then, the quick increase in the amount of fluorine released is assigned to the thermally activated cleavage of the C-F bonds, with a maximum of release around 350 °C. Above this temperature, a decrease of the measured intensity is observed, highlighting that all fluorine atoms were released; the quantity observed after 600 °C is due to the remanence of fluorine typical for $m/z = 19$.

Once again, no difference can be noted according to the plasma type; *i.e.* the fluorine release occurs in equal proportions for the two gases. Thereby, fibers treated with C_2F_5H do not emit more CF_3 than those fluorinated with CF_4 while NMR showed a higher CF_3 content in the second case. The CF_3 groups could decompose into F radicals via a C-F bond cleavage rather than CF_3 radical (C–C cleavage). Surprisingly, the total weight loss is slightly lower for the fluorinated fibers. The difference is around 370 °C when F and CF3 are emitted (after that the difference is maintained). The departure of fluorine in its F form can lead to a molecular reorganization that slightly stabilizes the residues; this phenomenon is nevertheless limited. The thermal behavior of the fibers is very slightly changed with plasma fluorination and the amount of fluorinated gases released is negligible.

3.4. Discussions

Pentafluoroethane as plasma gas precursor has been chosen by Xie *et al* [32] to treat the surface of wood (Golden chinkapin or *Castanopsis chrysophylla*) and achieve (super)hydrophobic properties. Wood and vegetal fibers are both composed of hemicelluloses, lignin and hemicellulose; only proportion of these latter varies depending on the species (Table 7). After a 2 min of fluorination (120 W, C_2F_5H/Ar flow rate = 20/75 SCCM), Xie *et al.* [32] have succeed to significantly reduce the hydrophobic character of wood, which exhibited then a water contact angle of 140.3 ± 2.2° to be compared with 98 ± 13° for our case of C_2F_5H-treated fibers. We have to pay attention that both values have not been obtained using the same condition, *i.e.* sessile drop for the wood and Wilhelmy balance for fibers, and that the experimental conditions are not necessarily comparable. However, the difference of 40° cannot be explained only by the techniques used, wood being probably "more reactive" in accordance with the higher content of lignin in Golden chinkapin than in flax fibers (Table 7). The flax fibers contain 2.9 + 0.9% of lignin, while, according to [73], 26% of lignin are present in *Castanopsis chrysophylla.* As demonstrated by Pouzet *et al.* [74], lignin is more reactive to F_2 than cellulose and hemicelluloses because both of its non-crystallinity and its high number of hydroxyl groups in its structure. Therefore, the same phenomenon is expected during the reaction with C_2F_5H plasma.

In any case, both wood and flax fibers treatment allows the polarity of the natural substrates to be significantly reduced, demonstrating that the conclusion may be applied to all lignocellulosic compounds.

Table 7
Composition of flax fibers and general hardwood.

	Flax fibers (%) [34,35]	Hardwood % [75]
Lignin	2–3	18–32
Cellulose	60–81	38–56
Hemicelluloses	14–21	16–31
Extractives	<10	1–5

Direct fluorination, as well as plasma fluorination as evidenced in this paper, allows fluorine atoms to be covalently grafted on the surface of lignocellulosic materials such as wood [23,76] or plant fibers [43]. Therefore, a comparison between these processes have to be conducted, based on the paper [43].

On reaction mechanism first, direct fluorination is a solid–gas process based on the high reactivity of F_2 molecules which first dissociate into two F• and combine with the surface in a second step. Therefore, CHF, CF and CF_2 groups are first formed until all C-CH_2-C group are convert into C-CF_2-C group (perfluorination at this step). However, if the reaction goes further after this step, the formation of CF_3 groups is accompanied by the cleavage of C–C bonds in a process similar to a decomposition. When another fluorine atoms are added, C–C cleavage and release of CF_4 gas occur. This decomposition always takes place and etches the surface. These changes of the surface chemical composition were evidences by FTIR, NMR and XPS spectroscopies. The same phenomena of fluorination/decomposition occur with CF_4 based plasma on surface activated by Ar in the plasma while a continuous increase of CF_x contents is observed with C_2F_5H based plasma.

According to ^{19}F NMR data, the nature of the fluorinated layer is similar with first CF and CF_2 and then CF_3 (decomposition) for the cases of F_2 gas and CF_4 plasma. CF_4 based plasma dissociation necessarily generates $F^\bullet$ in large amount which will react in the same way as F_2 *via* dissociation which will also produce $F^\bullet$. On the contrary, C_2F_5H based plasma generate a large amount of different radicals, which induces a much more different reaction mechanism, but above all one that buffers the grade reactivity of $F^\bullet$ (species present in this plasma).

The main difference between plasma and direct fluorination concerns the thickness of the fluorinated layer formed that can be indirectly estimated by the pulse number in ^{19}F NMR measurements to acquire a spectrum with adequate signal-to-noise ratio (256 and 512 pulses, for fibers fluorinated with F_2 and plasma respectively); the thickness of the fluorinated layer is much lower after plasma fluorination. Here are compared the samples optimized in term of polar group content (the lowest as possible).

Despite lower thickness of the fluorinated layer after plasma treatment, a significant and similar decrease in the polarity of the fibers is achieved whatever the fluorinated gas (CF_4 or C_2F_5H). Whatever the reactive species in the plasma ($F^\bullet$ $CF_2^\bullet$, $CF_3^\bullet$ or $CF_3^\bullet$, $CF_2^\bullet$, $CF^\bullet$, $F^\bullet$, $CHF_2^\bullet$, $CHF^\bullet$ radicals for CF_4 and C_2F_5H based plasmas, respectively), when present on the surface of the fibers, fluorine atoms decrease the polarity of the fibers and allow these fibers to be compatibilized with mostly dispersive polymers.

Additionally, the main difference concerns the mechanical properties of fibers after treatment. Indeed, if after controlled direct fluorination, the Young's modulus is maintained and a decrease of the stress and the maximum strain at break, plasma fluorinated fibers exhibit a decrease of these 3 quantities, evidencing that the bulk of the fibers has been also affected by the treatment (probably due to the open porosity of the fibers).

However, the scale-up of the direct F_2 fluorination appears to be easier by increasing the size of the reactor. For both direct and plasma fluorination processes, continuous methods for which the fibers move under the F_2/N_2 flow or under a plasma torch as for polymer film treatment (*e.g.* corona treatment) will be required. If the scale-up is successful, both techniques offer good means to treat large samples for different industries (automotive, aerospace…).

4. Conclusion

For the first time, the plasma fluorination of flax fibers was achieved in order to decrease their polarity by grafting fluorinated groups mainly in substitution to COH groups.

A set of complementary techniques, *i.e.* FT-IR, XPS and NMR analyses, allowed to better understand the reaction mechanisms according

the two studied gases CF_4 and C_2F_5H. Contrary to the direct fluorination, plasma fluorination allows the surface chemistry to be tailored in particular the relative content of CF_3 groups according to the precursor gas. Whereas the roughness is also endured and not controlled with the direct fluorination, the etching due to Ar may be used to tailor the roughness in the plasma fluorination.

In terms of mechanical properties, the stress and strain at break decrease whatever the plasma type whereas the Young's modulus slightly decreases too.

The present study opens new perspectives for the use of plasma fluorination with firstly the investigation of other fluorinated gases to enlarge the possible surface chemistries, *e.g.* SF_6 is promising because SFx groups would be grafted. $CHClF_2$ is another candidate in order to investigated the role of chlorine atoms in the halogenation processes.

In any case, targeting greenhouse gases such as CF_4 or refrigerants such as C_2F_5H as plasma precursor would be a way to recover them at the end of their lifecycle. Hydrochlorofluorocarbons or HCFCs and chlorofluorocarbons (CFCs) used in refrigeration and air conditioning systems have high global warming potentials (GWPs); those of CF_4 and monochlorodifluoromethane (HCFC-22) are, respectively, 6,500 and 1,800 times higher than CO_2. Perfluorocarbons (PFCs) are used in the semiconductor industry, like SF_6 which is used as an electrical insulator in transformers. The circular economy approach of recycling these fluorinated gases in a fluorinated plasma is all the more relevant as it involves bio-sourced materials, especially natural fibers.

CRediT authorship contribution statement

Olivier Téraube: Conceptualization, Methodology, Software, Validation, Formal analysis, Investigation, Data curation, Writing – original draft, Visualization. **Léa Gratier:** Methodology, Software, Formal analysis, Investigation, Data curation, Visualization, Writing – review & editing. **Jean-Charles Agopian:** Formal analysis, Investigation, Writing – review & editing. **Monica Francesca Pucci:** Methodology, Validation, Resources, Writing – review & editing. **Pierre-Jacques Liotier:** Methodology, Validation, Resources, Writing – review & editing. **Samar Hajjar-Garreau:** Investigation, Resources, Writing – review & editing. **Elodie Petit:** Investigation, Resources, Writing – review & editing. **Nicolas Batisse:** Investigation, Validation, Resources, Writing – review & editing. **Angélique Bousquet:** Investigation, Validation, Resources, Writing – review & editing. **Karine Charlet:** Conceptualization, Methodology, Resources, Writing – review & editing, Supervision, Project administration. **Éric Tomasella:** Conceptualization, Methodology, Resources, Writing – review & editing, Supervision, Project administration. **Marc Dubois:** Conceptualization, Methodology, Resources, Writing – review & editing, Supervision, Project administration, Funding acquisition.

Declaration of Competing Interest

The authors declare that they have no known competing financial interests or personal relationships that could have appeared to influence the work reported in this paper.

Data availability

Data will be made available on request.

Appendix A. Supplementary material

Supplementary data to this article can be found online at https://doi.org/10.1016/j.apsusc.2022.155615.

References

[1] C. Baley, A. Bourmaud, P. Davies, Eighty years of composites reinforced by flax fibres: a historical review, Compos. Part A: Appl. Sci. Manuf. 144 (2021) 106333, https://doi.org/10.1016/j.compositesa.2021.106333.

[2] M.J. Mochane, T.C. Mokhena, T.H. Mokhothu, A. Mtibe, E.R. Sadiku, S.S. Ray, I. D. Ibrahim, O.O. Daramola, Recent progress on natural fiber hybrid composites for advanced applications: a review, Exp. Polym. Lett. 13 (2019) 159–198, https://doi.org/10.3144/expresspolymlett.2019.15.

[3] A. Lotfi, H. Li, D.V. Dao, G. Prusty, Natural fiber–reinforced composites: a review on material, manufacturing, and machinability, J. Thermoplast. Compos. Mater. 34 (2021) 238–284, https://doi.org/10.1177/0892705719844546.

[4] M.F. Pucci, P.-J. Liotier, D. Seveno, C. Fuentes, A. Van Vuure, S. Drapier, Wetting and swelling property modifications of elementary flax fibres and their effects on the Liquid Composite Molding process, Compos. Part A: Appl. Sci. Manuf. 97 (2017) 31–40, https://doi.org/10.1016/j.compositesa.2017.02.028.

[5] J. Müssig, N. Graupner, Test methods for fibre/matrix adhesion in cellulose fibre-reinforced thermoplastic composite materials: a critical review, in: K.L. Mittal (Ed.), Progress in Adhesion and Adhesives, 1st ed.,, Wiley, 2021, pp. 69–130, https://doi.org/10.1002/9781119846703.ch4.

[6] S.O. Amiandamhen, M. Meincken, L. Tyhoda, Natural fibre modification and its influence on fibre-matrix interfacial properties in biocomposite materials, Fibers Polym. 21 (2020) 677–689, https://doi.org/10.1007/s12221-020-9362-5.

[7] F.M. AL-Oqla, M.S. Salit, Natural fiber composites, in: Materials Selection for Natural Fiber Composites, Elsevier, 2017, pp. 23–48. <https://doi.org/10.1016/B978-0-08-100958-1.00002-5>.

[8] V.K. Thakur, M. Thakur, M.R. Kessler, Handbook of Composites from Renewable Materials, Scrivener Publishing LLC, 2017.

[9] L. Calabrese, V. Fiore, E. Piperopoulos, D. Badagliacco, D. Palamara, A. Valenza, E. Proverbio, In situ monitoring of moisture uptake of flax fiber reinforced composites under humid/dry conditions, J. Appl. Polym. Sci. 139 (2022) 51969, https://doi.org/10.1002/app.51969.

[10] A. Gholampour, T. Ozbakkaloglu, A review of natural fiber composites: properties, modification and processing techniques, characterization, applications, J. Mater. Sci. 55 (2020) 829–892, https://doi.org/10.1007/s10853-019-03990-y.

[11] A. Dong, X. Fan, Q. Wang, Y. Yu, A. Cavaco-Paulo, Hydrophobic surface functionalization of lignocellulosic jute fabrics by enzymatic grafting of octadecylamine, Int. J. Biol. Macromole. 79 (2015) 353–362, https://doi.org/10.1016/j.ijbiomac.2015.05.007.

[12] A. Dong, Y. Yu, J. Yuan, Q. Wang, X. Fan, Hydrophobic modification of jute fiber used for composite reinforcement via laccase-mediated grafting, Appl. Surf. Sci. 301 (2014) 418–427, https://doi.org/10.1016/j.apsusc.2014.02.092.

[13] V. Fiore, T. Scalici, F. Nicoletti, G. Vitale, M. Prestipino, A. Valenza, A new eco-friendly chemical treatment of natural fibres: effect of sodium bicarbonate on properties of sisal fibre and its epoxy composites, Compos. Part B: Eng. 85 (2016) 150–160, https://doi.org/10.1016/j.compositesb.2015.09.028.

[14] X. Huang, A. Wang, X. Xu, H. Liu, S. Shang, Enhancement of hydrophobic properties of cellulose fibers via grafting with polymeric epoxidized soybean oil, ACS Sust. Chem. Eng. 5 (2017) 1619–1627, https://doi.org/10.1021/acssuschemeng.6b02359.

[15] T. Kick, T. Grethe, B. Mahltig, A natural based method for hydrophobic treatment of natural fiber material, ACSi. 64 (2017) 373–380. https://doi.org/10.17344/acsi.2017.3232.

[16] K. Lee, J.S. Jur, D.H. Kim, G.N. Parsons, Mechanisms for hydrophilic/hydrophobic wetting transitions on cellulose cotton fibers coated using Al $_{2}$ O 3 atomic layer deposition, J. Vac. Sci. Technol. A: Vac. Surf. Films. 30 (2012) 01A163, https://doi.org/10.1116/1.3671942.

[17] K. Thakur, S. Kalia, D. Pathania, A. Kumar, N. Sharma, C.L. Schauer, Surface functionalization of lignin constituent of coconut fibers via laccase-catalyzed biografting for development of antibacterial and hydrophobic properties, J. Clean. Prod. 113 (2016) 176–182, https://doi.org/10.1016/j.jclepro.2015.11.048.

[18] Q. Wang, S. Xiao, S.Q. Shi, S. Xu, L. Cai, Self-bonded natural fiber product with high hydrophobic and EMI shielding performance via magnetron sputtering Cu film, Appl. Surf. Sci. 475 (2019) 947–952, https://doi.org/10.1016/j.apsusc.2019.01.059.

[19] A. Fridman, Plasma Chemistry, Cambridge University Press, 2008.

[20] M.M. Kouicem, E. Tomasella, A. Bousquet, N. Batisse, G. Monier, C. Robert-Goumet, L. Dubost, An investigation of adhesion mechanisms between plasma-treated PMMA support and aluminum thin films deposited by PVD, Appl. Surf. Sci. 564 (2021), 150322, https://doi.org/10.1016/j.apsusc.2021.150322.

[21] Y. Kusano, D.J.H. Cederløf, S. Fæster, Plasma surface modification of glass fibre sizing for manufacturing polymer composites, KEM. 843 (2020) 159–164, https://doi.org/10.4028/www.scientific.net/KEM.843.159.

[22] W.-H. Cheng, M.-T. Lee, K. Yasuda, J.-M. Song, Plasma-modified PI substrate for highly reliable laser-sintered copper films using Cu2O nanoparticles, Nanomaterials. 12 (2022) 3237, https://doi.org/10.3390/nano12183237.

[23] F. Saulnier, M. Dubois, K. Charlet, L. Frezet, A. Beakou, Direct fluorination applied to wood flour used as a reinforcement for polymers, Carbohydr. Polym. 94 (2013) 642–646, https://doi.org/10.1016/j.carbpol.2013.01.060.

[24] K. Charlet, F. Saulnier, D. Gautier, M. Pouzet, M. Dubois, A. Béakou, Fluorination as an effective way to reduce natural fibers hydrophilicity, in: R. Fangueiro, S. Rana (Eds.), Natural Fibres: Advances in Science and Technology Towards Industrial Applications, Springer, Netherlands, Dordrecht, 2016, pp. 211–229, https://doi.org/10.1007/978-94-017-7515-1_16.

[25] C. Cardinaud, Fluorine-based plasmas: main features and application in micro-and nanotechnology and in surface treatment, C R Chim. 21 (2018) 723–739.

[26] A.P. Kharitonov, G.V. Simbirtseva, A. Tressaud, E. Durand, C. Labrugère, M. Dubois, Comparison of the surface modifications of polymers induced by direct fluorination and rf-plasma using fluorinated gases, J. Fluor. Chem. 165 (2014) 49–60, https://doi.org/10.1016/j.jfluchem.2014.05.002.

[27] A. Ali, K. Shaker, Y. Nawab, M. Jabbar, T. Hussain, J. Militky, V. Baheti, Hydrophobic treatment of natural fibers and their composites—a review, J. Ind. Text. 47 (2018) 2153–2183, https://doi.org/10.1177/1528083716654468.

[28] S.G. Lee, S.-S. Choi, W.H. Park, D. Cho, Characterization of surface modified flax fibers and their biocomposites with PHB, Macromol. Symp. 197 (2003) 089–100.

[29] A. Sparavigna, Plasma treatment advantages for textiles, 2008.

[30] D. Sun, G.K. Stylios, Fabric surface properties affected by low temperature plasma treatment, J. Mater. Process. Technol. 173 (2006) 172–177, https://doi.org/10.1016/j.jmatprotec.2005.11.022.

[31] Y. Han, S.O. Manolach, F. Denes, R.M. Rowell, Cold plasma treatment on starch foam reinforced with wood fiber for its surface hydrophobicity, Carbohydr. Polym. 86 (2011) 1031–1037, https://doi.org/10.1016/j.carbpol.2011.05.056.

[32] L. Xie, Z. Tang, L. Jiang, V. Breedveld, D.W. Hess, Creation of superhydrophobic wood surfaces by plasma etching and thin-film deposition, Surf. Coat. Tech. 281 (2015) 125–132, https://doi.org/10.1016/j.surfcoat.2015.09.052.

[33] P.J. Van Soest, Use of detergents in the analysis of fibrous feeds. II. A rapid method for the determination of fiber and lignin, J. Assoc. Agric. Chem. 46 (1963) 829–835.

[34] A. Moudood, A. Rahman, A. Öchsner, M. Islam, G. Francucci, Flax fiber and its composites: an overview of water and moisture absorption impact on their performance, J. Reinf. Plast. Compos. 38 (2019) 323–339, https://doi.org/10.1177/0731684418818893.

[35] V. Dhyani, T. Bhaskar, Pyrolysis of Biomass, in: Biofuels: Alternative Feedstocks and Conversion Processes for the Production of Liquid and Gaseous Biofuels, Second edition, Elsevier, 2019, pp. 217–244.

[36] S. Ibrahim, P. Bonnet, M. Sarakha, C. Caperaa, G. Monier, A. Bousquet, Tailoring the structural and optical properties of bismuth oxide films deposited by reactive magnetron sputtering for photocatalytic application, Mater. Chem. Phys. 243 (2020), 122580, https://doi.org/10.1016/j.matchemphys.2019.122580.

[37] S. Ibrahim, Synthesis of Bismuth-Based Thin Films and Nanoparticles by Reactive Magnetron Sputtering for Photocatalytic Applications, Université Clermont Auvergne, 2020.

[38] T. Young, An essay on the cohesion of fluids, Philos. Trans. Roy. Soc. London. 95 (1805) 65–87.

[39] S.L. Schellbach, S.N. Monteiro, J.W. Drelich, A novel method for contact angle measurements on natural fibers, Mater. Lett. 164 (2016) 599–604, https://doi.org/10.1016/j.matlet.2015.11.039.

[40] S. Qiu, C.A. Fuentes, D. Zhang, A.W. Van Vuure, D. Seveno, Wettability of a single carbon fiber, Langmuir. 32 (2016) 9697–9705.

[41] A. Hodzic, Z.H. Stachurski, Droplet on a fibre: Surface tension and geometry, Compos. Interf. 8 (2001) 415–425, https://doi.org/10.1163/156855401753424451.

[42] J.M. Van Hazendonk, J.C. Van der Putten, J.T.F. Keurentjes, A. Prins, A simple experimental method for the measurement of the surface tension of cellulosic fibres and its relation with chemical composition, Colloids Surf. A: Physicochem. Eng. Aspects. 81 (1993) 251–261.

[43] O. Téraube, J.-C. Agopian, M.F. Pucci, P.-J. Liotier, S. Hajjar-Garreau, N. Batisse, K. Charlet, M. Dubois, Fluorination of flax fibers for improving the interfacial compatibility of eco-composites, SM&T. (2022) e00467.

[44] D.K. Owens, R.C. Wendt, Estimation of the surface free energy of polymers, J. Appl. Polym. Sci. 13 (1969) 1741–1747, https://doi.org/10.1002/app.1969.070130815.

[45] A. Roudier, K. Charlet, F. Moreno, E. Toussaint, C. Géneau-Sbartaï, S. Commereuc, V. Verney, A. Béakou, Caractérisation des propriétés biochimiques et hygroscopiques d'une fibre de lin, Matér. Tech. 100 (2012) 525–535, https://doi.org/10.1051/mattech/2012044.

[46] G. Socrates, Infrared and Raman Characteristic Group Frequencies: Tables and Charts, third ed., Wiley, Chichester; New York, 2001.

[47] S. Sapieha, M. Verreault, J.E. Klemberg-Sapieha, E. Sacher, M.R. Wertheimer, X-Ray photoelectron study of the plasma fluorination of lignocellulose, Appl. Surf. Sci. 44 (1990) 165–169.

[48] B. Ly, M.N. Belgacem, J. Bras, M.C. Brochier Salon, Grafting of cellulose by fluorine-bearing silane coupling agents, Mater. Sci. Eng.: C. 30 (2010) 343–347, https://doi.org/10.1016/j.msec.2009.11.009.

[49] A. Tursi, N. De Vietro, A. Beneduci, A. Milella, F. Chidichimo, F. Fracassi, G. Chidichimo, Low pressure plasma functionalized cellulose fiber for the remediation of petroleum hydrocarbons polluted water, J. Hazard. Mater. 373 (2019) 773–782, https://doi.org/10.1016/j.jhazmat.2019.04.022.

[50] G. Beamson, G. Briggs, High resolution XPS of organic polymers: the scienta ESCA300 database, J. Chem. Educ. 70 (1993) A25, https://doi.org/10.1021/ed070pA25.5.

[51] B. Rousseau, H. Estrade-Szwarckopf, Photoelectron core level spectroscopy study of K- and Rb-graphite intercalation compounds –II. Clean surfaces study, Solid State Commun. 85 (1993) 793–797, https://doi.org/10.1016/0038-1098(93)90673-B.

[52] R.H. Dastur, J.G. Bhatt, Relation of potassium to fusarium wilt of flax, Nature. 201 (1964) 1243–1244, https://doi.org/10.1038/2011243a0.

[53] B. Khiari, A. Ibn Ferjani, A.A. Azzaz, S. Jellali, L. Limousy, M. Jeguirim, Thermal conversion of flax shives through slow pyrolysis process: in-depth biochar characterization and future potential use, Biomass Conv. Bioref. 11 (2021) 325–337, https://doi.org/10.1007/s13399-020-00641-0.

[54] A.P. Kharitonov, Direct Fluorination of Polymers, Nova Publishers (2008).

[55] A.P. Kharitonov, R. Taege, G. Ferrier, V.V. Teplyakov, D.A. Syrtsova, G.-H. Koops, Direct fluorination—useful tool to enhance commercial properties of polymer articles, J. Fluor. Chem. 126 (2005) 251–263, https://doi.org/10.1016/j.jfluchem.2005.01.016.

[56] A.P. Kharitonov, R. Taege, G. Ferrier, N.P. Piven, The kinetics and mechanism of the direct fluorination of polyethylenes, Surf. Coat. Int. Part B: Coat. Trans. 88 (2005) 201–212, https://doi.org/10.1007/BF02699574.

[57] M. Suto, L.C. Lee, Emission spectra of CF_3 radicals. V. Photodissociation of CF_3H, CF_3Cl, and CF_3Br by vacuum ultraviolet, J. Chem. Phys. 79 (1983) 1127–1133, https://doi.org/10.1063/1.445914.

[58] S. Agraharam, D.W. Hess, P.A. Kohl, S.A.B. Allen, Plasma chemistry in fluorocarbon film deposition from pentafluoroethane/ argon mixtures, J. Vac. Sci. Technol. A. 17 (1999) 3265–3271.

[59] A.P. Kharitonov, Practical applications of the direct fluorination of polymers, J. Fluor. Chem. 103 (2000) 123–127, https://doi.org/10.1016/S0022-1139(99)00312-7.

[60] M. Pouzet, M. Dubois, K. Charlet, A. Béakou, From hydrophilic to hydrophobic wood using direct fluorination: a localized treatment, C. R. Chim. 21 (2018) 800–807, https://doi.org/10.1016/j.crci.2018.03.009.

[61] A. Tressaud, Fluorine, a key element for the 21st century, in: Fluorine, Elsevier, 2019, pp. 77–150. <https://doi.org/10.1016/B978-0-12-812990-6.00002-7>.

[62] V. Satulu, M. Ionita, S. Vizireanu, B. Mitu, G. Dinescu, Plasma processing with fluorine chemistry for modification of surfaces wettability, Molecules. 21 (2016) 1711, https://doi.org/10.3390/molecules21121711.

[63] L. Lin, L. Rui, Y. Tao, Q. Li, W.-H. Chiang, H. Xu, Surface modification of metal substrates using dielectric barrier discharge plasma and the wettability study, J. Taiwan Inst. Chem. Eng. 138 (2022), 104467, https://doi.org/10.1016/j.jtice.2022.104467.

[64] K. Charlet, C. Baley, C. Morvan, J.P. Jernot, M. Gomina, J. Bréard, Characteristics of Hermès flax fibres as a function of their location in the stem and properties of the derived unidirectional composites, Compos. Part A: Appl. Sci. Manuf. 38 (2007) 1912–1921, https://doi.org/10.1016/j.compositesa.2007.03.006.

[65] M.J.P. Macedo, A.L.A. Mattos, T.H.C. Costa, M.C. Feitor, E.N. Ito, J.D.D. Melo, Effect of cold plasma treatment on recycled polyethylene/kapok composites interface adhesion, Compos. Interf. 26 (2019) 871–886, https://doi.org/10.1080/09276440.2018.1549892.

[66] P. Valášek, M. Müller, V. Šleger, Influence of plasma treatment on mechanical properties of cellulose-based fibres and their interfacial interaction in composite systems, BioResources. 12 (2017) 5449–5461. https://doi.org/10.15376/biores.12.3.5449-5461.

[67] F.S. Corral, L.A.C. Nava, E.H. Hernández, J.F.H. Gámez, M.G.N. Velázquez, M.I. M. Sierra, P.G. Morones, R.E.D.D.L. Gómez, Plasma treatment of *Agave* fiber powder and its effect on the mechanical and thermal properties of composites based on polyethylene, Int. J. Polym. Sci. (2016) 1–7, https://doi.org/10.1155/2016/2807915.

[68] T. Scalici, V. Fiore, A. Valenza, Effect of plasma treatment on the properties of Arundo Donax L. leaf fibres and its bio-based epoxy composites: a preliminary study, Compos. Part B: Eng. 94 (2016) 167–175, https://doi.org/10.1016/j.compositesb.2016.03.053.

[69] O. Teraube, J.-C. Agopian, E. Petit, F. Metz, N. Batisse, K. Charlet, M. Dubois, Surface modification of sized vegetal fibers through direct fluorination for eco-composites, J. Fluor. Chem. 238 (2020), 109618, https://doi.org/10.1016/j.jfluchem.2020.109618.

[70] R.A. Donaton, F. Iacopi, R. Baklanov, D. Shamiryan, B. Coenegrachts, H. Struyf, M. Lepage, M. Meuris, M. van Hove, W.D. Gray, H. Meynen, D. de Roest, S. Vanhaelemeersch, K. Maex, Physical and electrical characterization of silsesquioxane-based ultra-low k dielectric films, in: Proceedings of the IEEE 2000 International Interconnect Technology Conference (Cat. No.00EX407), IEEE, Burlingame, CA, USA, 2000, pp. 93–95. <https://doi.org/10.1109/IITC.2000.854292>.

[71] G.S. Mathad, H.S. Rathore, Copper Interconnects, New Contact Metallurgies/structures, and Low-k Interlevel Dielectrics: Proceedings of the International Symposium, The Electrochemical Society, 2001. <https://books.google.fr/books?id=zFax_C2Z4k8C&printsec=frontcover&hl=fr#v=onepage&q&f=false>.

[72] P.-J. Liotier, M.F. Pucci, A. Le Duigou, A. Kervoelen, J. Tirilló, F. Sarasini, S. Drapier, Role of interface formation versus fibres properties in the mechanical behaviour of bio-based composites manufactured by Liquid Composite Molding processes, Compos. Part B: Eng. 163 (2019) 86–95, https://doi.org/10.1016/j.compositesb.2018.10.103.

[73] E.F. Kurth, The chemical analysis of Western Woods. Part III, Tappi. 33 (1950) 507–508.

[74] M. Pouzet, M. Dubois, K. Charlet, A. Béakou, The effect of lignin on the reactivity of natural fibres towards molecular fluorine, Mater. Des. 120 (2017) 66–74, https://doi.org/10.1016/j.matdes.2017.01.086.

[75] D. Fengel, G. Wegener, 3. Chemical Composition and Analysis of Wood, in: Wood: Chemistry, Ultrastructure, Reactions, New York: De Gruyter, Berlin, 2011, pp. 26–65. <https://doi.org/10.1515/9783110839654.26>.

[76] M. Pouzet, M. Dubois, K. Charlet, A. Béakou, J.-M. Leban, M. Bada, Fluorination renders the wood surface hydrophobic without any loss of physical and mechanical properties 133 (2019) 133–141. <https://doi.org/10.1016/j.indcrop.2019.02.044>.